Scientific Research Publishing

Materials Sciences and Applications, 2019, 10, 216-226
http://www.scirp.org/journal/msa
ISSN Online: 2153-1188
ISSN Print: 2153-117X

Nanostructure of Rutile TiO_2 Thin Films Prepared on Unheated Substrate by Dual Cathode DC Unbalanced Magnetron Sputtering

Wichai Kongsri[1*], Supanee Limsuwan[1], Surasing Chaiyakun[2], Pichet Limsuwan[1], Chittra Kedkaew[1]

[1]Department of Physics, Faculty of Science, King Mongkut's University of Technology Thonburi, Bangkok, Thailand
[2]Department of Physics, Faculty of Science, Burapha University, Chonburi, Thailand
Email: *wichai973@yahoo.com, owikko@gmail.com, s-chaikhun@hotmail.com

How to cite this paper: Kongsri, W., Limsuwan, S., Chaiyakun, S., Limsuwan, P. and Kedkaew, C. (2019) Nanostructure of Rutile TiO_2 Thin Films Prepared on Unheated Substrate by Dual Cathode DC Unbalanced Magnetron Sputtering. *Materials Sciences and Applications*, **10**, 216-226.
https://doi.org/10.4236/msa.2019.103018

Received: February 5, 2019
Accepted: March 22, 2019
Published: March 25, 2019

Abstract

In this work, structural and optical properties of the TiO_2 films deposited on unheated substrates by dual cathode dc unbalanced magnetron sputtering at long substrate-target distance (d_{s-t}) were studied. Titanium dioxide (TiO_2) thin films were deposited on unheated Si (110) wafers, glass slides and carbon coated copper grids at different substrate to target (d_{s-t}) distances. The structural properties of TiO_2 thin films were characterized by X-ray diffraction (XRD) and transmission electron microcopy (TEM) with selected-area electron diffraction (SAED), surface morphology using atomic force microscopy (AFM) and optical transmission spectra using a spectrophotometer. XRD results show that TiO_2 films deposited at various d_{s-t} distances have only rutile crystal structure. The crystallinity and thickness of the films increased while the roughness decreased with decreasing d_{s-t} distance. The refractive indices of the deposited films were found to be in the range of 2.51 - 2.82 and increased with decreasing d_{s-t} distance.

Keywords

TiO_2, Magnetron Sputtering, Rutile

1. Introduction

During the past two decades, nanocrystalline titanium dioxide (TiO_2) thin films have attracted a great deal of interest due to their photocatalytic properties and photoinduced superhydrophilicity [1] [2] [3] [4].

In general, TiO_2 exists in both crystalline and amorphous forms. Crystalline TiO_2 exists in three different phases: anatase, rutile and brukite. Anatase and

brookite are stable at the temperature below 600˚C and the anatase phase completely transforms to the rutile phase at the temperature above 750˚C [5]. The anatase phase is suitable for photocatalytic activities and superhydrophilic properties, white the rutile phase is widely used for optical applications [1]-[8].

TiO_2 thin films can be prepared by many methods, such as chemical vapor deposition, electron beam evaporation, ion beam assisted deposition, spray pyrolysis, sol-gel process and sputtering [1]-[14]. However, most of the TiO_2 films prepared by the above-mentioned methods are either amorphous or anatase. Among these methods, the reactive magnetron sputtering is one of the most widely used methods for the deposition of TiO_2 thin films. As reported in the literature, the TiO_2 films deposited on unheated substrates by dc reactive magnetron sputtering often exhibit an amorphous phase. Therefore, to obtain the rutile phase, the films have to be heated during or after the deposition at a high temperature above 600˚C [2] [8] [14] [15] [16] [17] [18].

Very few studies report on the deposition of TiO_2 thin films on unheated substrates by dc reactive magnetron sputtering [12] [13] [19]. In addition, the deposited TiO_2 films reported by those investigators were carried out at a relatively short-substrate distance in the range of 15 to 40 mm.

In this work, the rutile TiO_2 films were prepared on unheated substrates by a home built dual cathode dc unbalanced magnetron sputtering. The effect of the substrate-target distance ($d_{s\text{-}t}$) on the structural and optical properties of the TiO_2 films was studied.

2. Experimental Procedure

2.1. Sputtering Apparatus

Figure 1 shows the schematic diagram of dual-cathode dc unbalanced magnetron sputtering constructed in our laboratory. The magnetron sputtering cathodes consist of a coating cathode and an enhancing plasma cathode. The vacuum chamber has a diameter of 35 cm and a height of 38 cm. Two separated dc power supplies were used to supply each cathode independently. However, in this work only coating cathode was used for sputtering the Ti target and, hence, enhancing plasma cathode was closed by the shutter.

The maximum distance from the substrate to the target of coating cathode ($d_{s\text{-}t}$) was about 14 cm. The substrate holder can be rotated with an angular velocity from 10 - 200 rpm. The base pressure of the vacuum chamber was 1.0×10^{-5} mbar.

Figure 2 shows the schematic diagram of each magnetron sputtering cathode. A magnetron sputtering cathode consists of the magnetron body with two holes and two permanent magnets inside the magnetron body. The poles of both magnets were attached with the iron steel plate which hold on the magnetron body surface. The central magnet has a cylindrical shape with a diameter of 15 mm and a thickness of 15 mm. The outer magnet is a ring magnet with the inner and outer diameters of 53 and 83 mm, respectively. The magnetic field strength

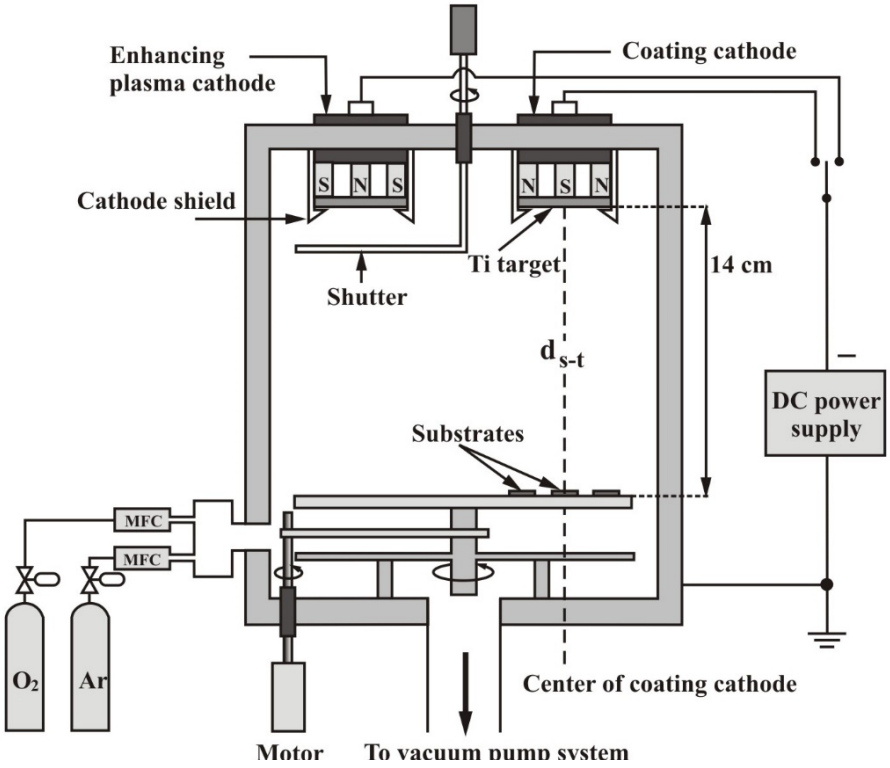

Figure 1. Schematic diagram of dual-cathode dc unbalanced magnetron sputtering.

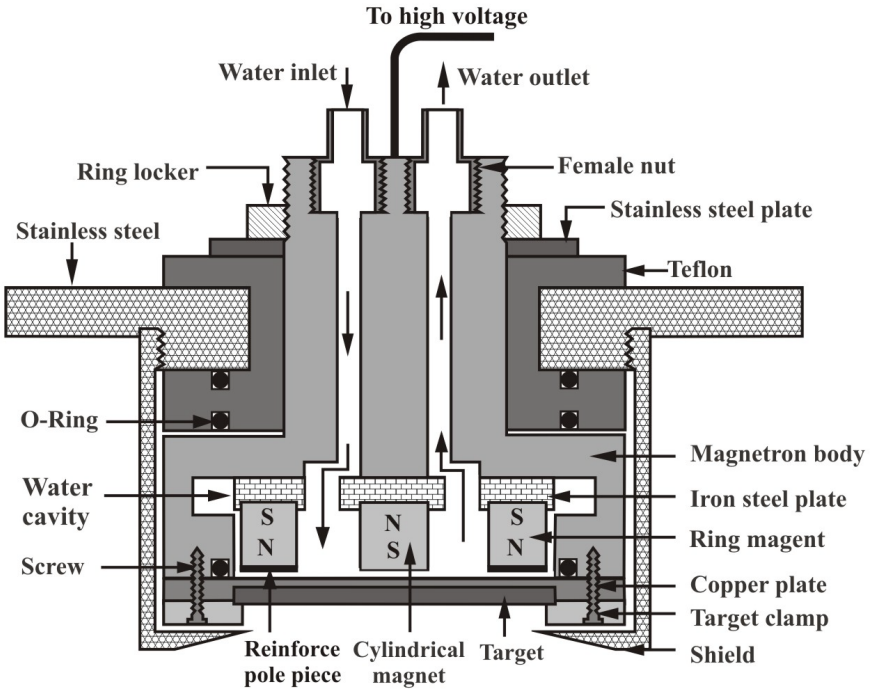

Figure 2. Magnetron sputtering cathode.

of both magnets was about 5000 G. Two holes with cavity inside the magnetron body were made for the water cooling of the sputtering target. The sputtering target was attached on the copper plate which contacted directly with the cooling

water.

Both cathodes are the same and installed in the vacuum chamber (Figure 1). However, in this work only the coating cathode was used and; hence, the other one behaves as enhancing plasma cathode. The study allows explanation into the possible effect of magnetic field on the rate of deposition and the phase formation of the deposited thin film, since the enhancing cathode alters the magnetic field strength of the system.

Figure 3 shows the magnetic field lines of dual-cathode unbalanced magnetron sputtering before it was installed in the vacuum chamber. The magnetic field lines are a combination of transverse and perpendicular components of the magnetic field. The magnetic field strength was also measured at different $d_{s\text{-}t}$ distances from coating cathode using a teslameter (PHYWE). The magnetic field strengths at the center and the side of target surface were measured to be 1700 and 1330 G, respectively.

2.2. Sample Preparation

The metallic titanium disc with a purity of 99.97% (Kurt J. Lesker) and 54 mm diameter was used as sputtering target. The Ar (99.999%, TIG) and O_2 (99.999%, TIG) were used as sputtering gas and reactive gas whose flow rates were controlled with the mass flow meters (MKS) at 1 and 4 sccm, respectively. Prior to sputtering, the chamber was evacuated to a base pressure of lower than 1.0×10^{-5} mbar and pre-sputtered for 5 min to clear out impure gases in the chamber

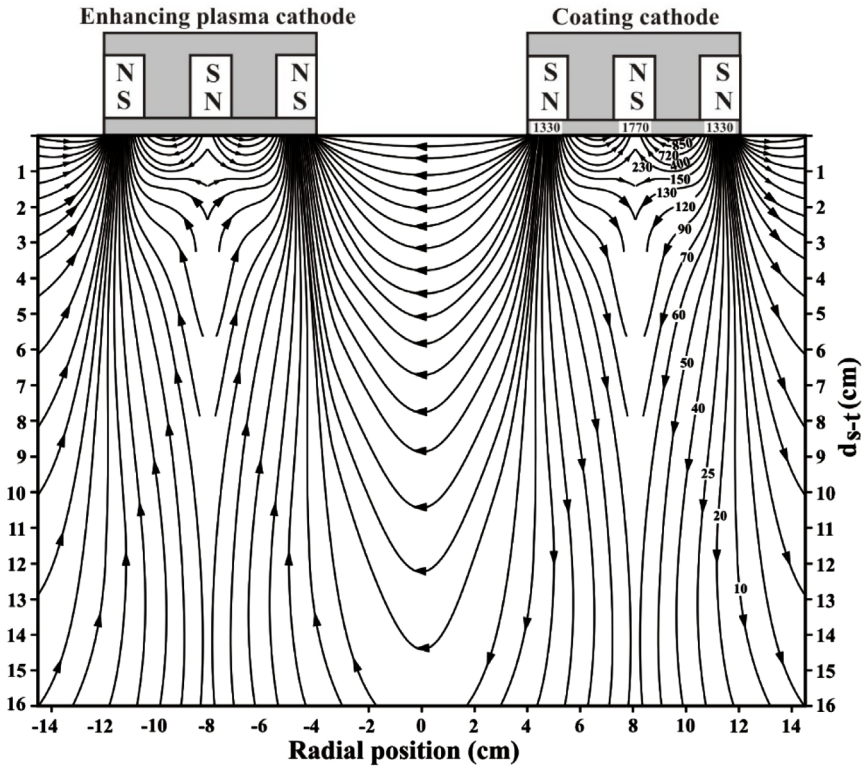

Figure 3. Magnetic field lines of dual-cathode unbalanced magnetron sputtering.

and remove other foreign elements on the titanium disc surface. The films were deposited at different d_{s-t} distances of 6, 8, 10 and 12 cm for 120 min. During sputtering, the pressure and dc power were kept constant at 5.0×10^{-3} mbar and 250 W, respectively.

The substrates used were glass slides for surface roughness analysis and optical transmission measurement, carbon coated copper grids for microstructure analysis and silicon (110) wafers for crystal structure analysis.

2.3. Characterization

The structure of the films was characterized by X-ray diffraction technique in thin film mode (TF-XRD, Rigaku, RINT-2100) adjusted with CuKα radiation, 40 kV, 40 mA at a step of $2\theta = 2^\circ$ min-1 and a 3˚ glancing angle against the incident beam in the 2θ range of 20˚ - 65˚. The crystal orientation of the films was investigated by transmission electronmicroscopy (TEM, Jeol JEM-2100) working at 160 kV. An atomic force microscopy (AFM, Veeco) was achieved with a Digital Instruments Nanoscope IV in a tapping mode for observation of the surface roughness, and film thickness. The optical transmission measurements of the films were carried out at room temperature using a UV-VIS spectrophotometer (Bruker, D8 Advance) in the wavelength range from 400 to 750 nm. Then, the refractive index (n) was calculated from optical transmission of the films using the Swanepoel's method [20].

3. Results and Discussion

Figure 4 shows the XRD-patterns of TiO_2 thin films deposited at different d_{s-t} distances of 6, 8, 10 and 12 cm. A single phase of rutile was clearly observed and could be indexed as R (110) plane according to JCPDS file No. 88-1175. Moreover, the crystallinity of rutile increased with decreasing d_{s-t} distances. This is because the magnetic field strength of the dual magnetron cathode is higher than

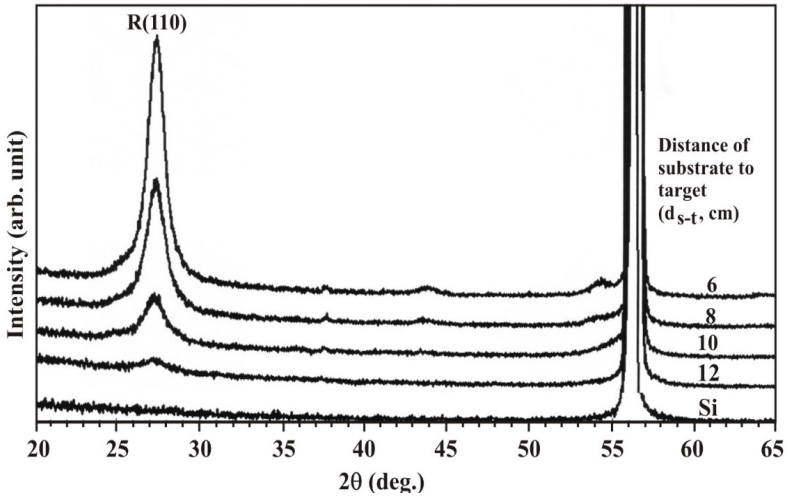

Figure 4. XRD patterns of TiO_2 films deposited by dual cathode at various d_{s-t} distances.

that of single magnetron cathode. The increase in magnetic field strength result in the increase of plasma as shown in Figure 5.

The rutile is a result of the reaction between decelerate Ti^+ species or activated Ti atoms and ions [21]. Generally, the electrons generated during the sputtering of coating cathode could be trapped in an unbalanced magnetic field (UMF), which results in a plasma being directed onto the substrate surface and relatively low voltage ion bombardment of the growing film surface due to self-bias potential [22]. The number of electrons was increased when the enhancing plasma cathode was installed, due to increasing the UMF [23]. The Ti^+ ions, which ionized by the electron impact on the Ti atoms, were increased and resulting in the increase of the probability of rutile formation [24] [25] [26]. The increase of crystallinity of rutile with the decrease of $d_{s\text{-}t}$ is the result of increasing the concentration of Ti^+ species and deposition energy. Normally, in a sputtering process, the sputter atoms are deposited on the substrate with kinetic energy in thermodynamically exception the potential energy [27]. Kinetic energy is the reciprocal of $d_{s\text{-}t}$ due to diminution of kinetic energy the impacting the sputtered atoms with other atoms in the deposition chamber. Inaddition, the high electron concentration in the magnetron sputtering was exhibited around the target face because of the high magneticfield strength. Thus, the high concentration of Ti^+ species is probably around the entire target face.

The surface root mean square roughness (R_{rms}) of the films deposited at different $d_{s\text{-}t}$ distances of 6, 8, 10 and 12 cm was determined from AFM images and the results are shown in Figure 6. The thickness of films was measured from the

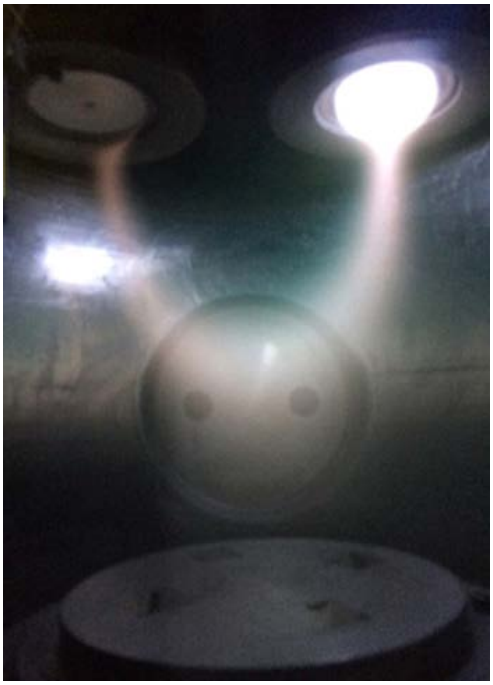

Figure 5. Photo of the Ar gas plasma at a pressure of 2.0×10^{-3} mbar and a sputtering power of 250 W.

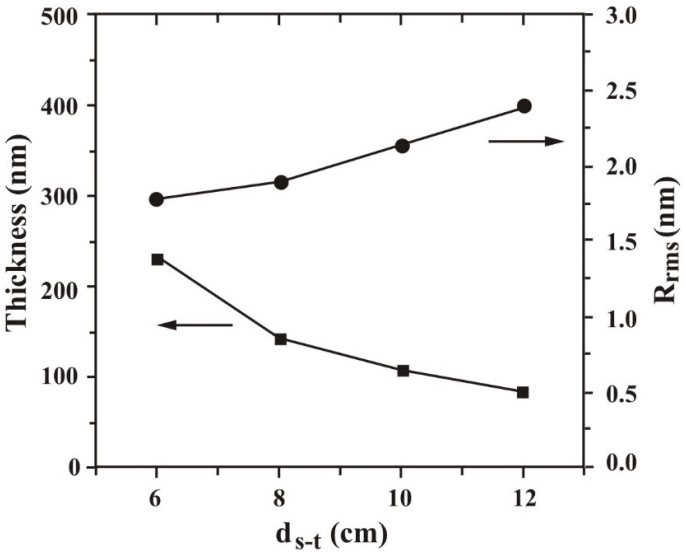

Figure 6. Thickness and surface root mean square roughness (R_{rms}) of TiO_2 films deposited by dual cathode at various ds-t distances.

section analysis of 2D-AFM images and the results are also shown in **Figure 6**. The grain size of the films was estimated from 2D-AFM images and the results were found to be 52.0, 43.3, 40.1 and 30.4 nm for d_{s-t} distances of 6, 8, 10 and 12 cm, respectively. It is seen that the roughness decreases with increasing distance as the effect of low kinetic energy of Ti particles. Kinetic energy is seen as the reciprocal of d_{s-t} due to diminution of kinetic energy by impacting of the sputtered atoms with other atoms in the deposition chamber.

The high-resolution transmission electron microscopy (HRTEM) images accompanied with the corresponding SAED patterns of films are shown in **Figure 7**. The observable lattice fringes and the distances of the fringe are measured to be 0.32 nm which corresponds well to the standard data (JCPDS 88-1175) in the (110) plane (d = 0.32 nm) of TiO_2 rutile phase. Moreover, the corresponding SAED patterns of films show the further planes of (101) and (211) rutile in the films deposited at d_{s-t} distances of 6, 8 and 10 cm, whereas only (110) plane is observed in the film deposited at the d_{s-t} distance of 12 cm due to the decrease of deposition energy when the d_{s-t} distance is increased.

The high-resolution transmission electron microscopy (HRTEM) images accompanied with the corresponding SAED patterns of films are shown in **Figure 7**. The observable lattice fringes and the distances of the fringe are measured to be 0.32 nm which corresponds well to the standard data (JCPDS 88-1175) in the (110) plane (d = 0.32 nm) of TiO_2 rutile phase. Moreover, the corresponding SAED patterns of films show the further planes of (101) and (211) rutile in the films deposited at d_{s-t} distances of 6, 8 and 10 cm, whereas only (110) plane is observed in the film deposited at the d_{s-t} distance of 12 cm due to the decrease of deposition energy when the d_{s-t} distance is increased.

Figure 8 shows the refractive indices in the wavelength from 400 - 750 nm of the deposited films as calculated from the optical transmission spectra using

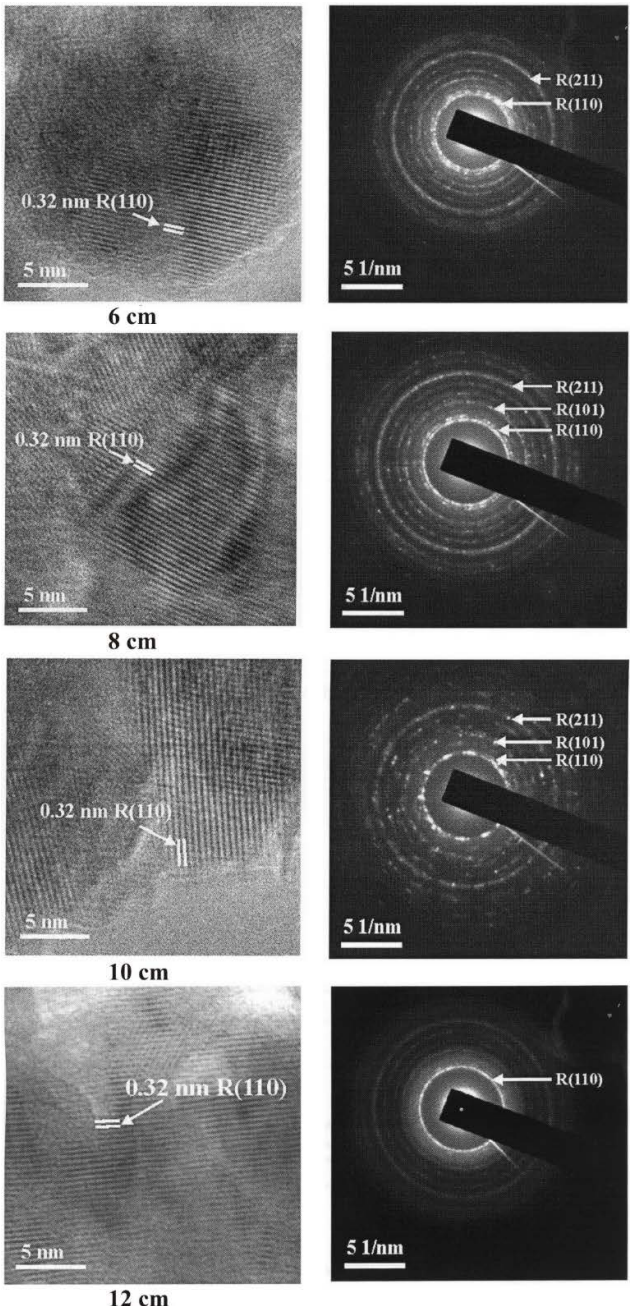

Figure 7. (a) HRTEM images and (b) SAED images of TiO_2 films deposited at various d_{s-t} distances.

Swanepoel's method. The refractive indices were found to be in the range of 2.51 - 2.82. The high refractive index was observed on films deposited at a low d_{s-t} distance. Generally, the refractive index is proportional to the crystallinity of films. Therefore, the higher crystallinity of film deposited at d_{s-t} distance of 6 cm exhibited the high refractive index.

4. Conclusion

The rutile TiO_2 films were deposited on unheated Si (110) wafers, glass slides

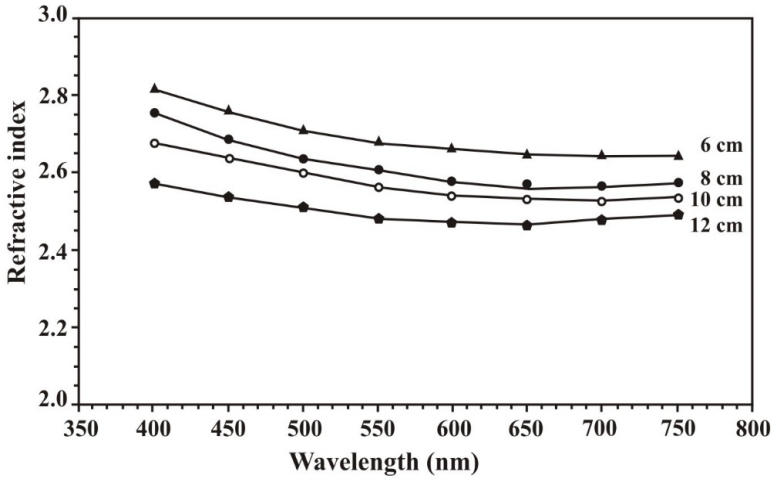

Figure 8. Refractive index (n) of TiO_2 films deposited at various d_{s-t} distances.

and carbon coated copper grids at different substrate to target distances (d_{s-t}) of 6, 8, 10 and 12 cm. The rutile phase was observed for all films deposited in the d_{s-t} range of 6 - 12 cm. The formation of rutile phase even on the unheated substrates is due to high magnetic field strength from dual magnetron cathode which enhances the plasma inside the vacuum chamber. The results from this work confirm that the magnetron cathode constructed and used for the deposition of TiO_2 thin films is suitable for the fabrication of crystalline films without heating the substrates. Further studies into detail mechanism and controlling of the TiO_2 phase formation is interesting topic for unheated substrates deposition system.

Fund

This work was supported by King Mongkut's University of Technology Thonburi under National Research University Project.

Conflicts of Interest

The authors declare no conflicts of interest regarding the publication of this paper.

References

[1] Zeman, P. and Takabayashi, S. (2002) Effect of Total and Oxygen Partial Pressures on Structure of Photocatalytic TiO_2 Films Sputtered on Unheated Substrate. *Surface and Coatings Technology*, **153**, 93-99. https://doi.org/10.1016/S0257-8972(01)01553-5

[2] Zheng, S.K., Wang, T.M., Xiang, G. and Wang, C. (2001) Photocatalytic Activity of Nanostructured TiO_2 Thin Films Prepared by DC Magnetron Sputtering Method. *Vacuum*, **62**, 361-366. https://doi.org/10.1016/S0042-207X(01)00353-0

[3] Zeman, P. and Takabayashi, S. (2003) Nano-Scaled Photocatalytic TiO_2 Thin Films Prepared by Magnetron Sputtering. *Thin Solid Films*, **433**, 57-62. https://doi.org/10.1016/S0040-6090(03)00311-0

[4] Song, P.K., Irie, Y., Sato, Y. and Shigesato, Y. (2004) Crystal Structure and Photocatalytic Activity of TiO_2 Films Deposited by Reactive Sputtering Using Ne, Ar, Kr, or Xe Gases. *Japanese Journal of Applied Physics*, **43**, L358. https://doi.org/10.1143/JJAP.43.L358

[5] Zhang, I., Li, M., Feng, Z., Chen, J. and Li, C. (2006) UV Raman Spectroscopic Study on TiO_2. I. Phase Transformation at the Surface and in the Bulk. *The Journal of Physical Chemistry B*, **110**, 927-935. https://doi.org/10.1021/jp0552473

[6] Reidy, D.J., Holmes, J.D. and Morris, M.A. (2006) Preparation of a Highly Thermally Stable Titania Anatase Phase by Addition of Mixed Zirconia and Silica Dopants. *Ceramics International*, **32**, 235-239. https://doi.org/10.1016/j.ceramint.2005.02.009

[7] Sumita, T., Otsuka, H., Kubota, H., Nagata, M., Honda, Y., Miyagawa, R., Tsurushima, T. and Sadoh, T. (1999) Ion-Beam Modification of TiO_2 Film to Multilayered Photocatalyst. *Nuclear Instruments and Methods in Physics Research Section B: Beam Interactions with Materials and Atoms*, **148**, 758-761. https://doi.org/10.1016/S0168-583X(98)00809-X

[8] Karunagaran, B., Kumar, R.T., Kumar, V.S., Mangalaraj, D., Narayandass, S.K. and Rao, G.M. (2003) Structural Characterization of DC Magnetron-Sputtered TiO_2 Thin Films Using XRD and Raman Scattering Studies. *Materials Science in Semiconductor Processing*, **6**, 547-550. https://doi.org/10.1016/j.mssp.2003.05.012

[9] Miao, L., Jin, P., Kaneko, K., Terai, A., Gabain, N. and Tanemura, S. (2003) Preparation and Characterization of Polycrystalline Anatase and Rutile TiO_2 Thin Films by RF Magnetron Sputtering. *Applied Surface Science*, **212-213**, 255-263. https://doi.org/10.1016/S0169-4332(03)00106-5

[10] Buscema, C.L., Malibert, C. and Bach, S. (2002) Elaboration and Characterization of Thin Films of TiO_2 Prepared by Sol-Gel Process. *Thin Solid Films*, **418**, 79-84. https://doi.org/10.1016/S0040-6090(02)00714-9

[11] Bhattacharyya, D., Sahoo, N.K., Thakur, S. and Das, N.C. (2000) Spectroscopic Ellipsometry of TiO_2 Layers Prepared by Ion-Assisted Electron-Beam Evaporation. *Thin Solid Films*, **360**, 96-102. https://doi.org/10.1016/S0040-6090(99)00966-9

[12] Meng, L.J. and Santos, M.P. (1993) Investigations of Titanium Oxide Films Deposited by D.C. Reactive Magnetron Sputtering in Different Sputtering Pressures. *Thin Solid Films*, **226**, 22-29. https://doi.org/10.1016/0040-6090(93)90200-9

[13] Toku, H., Pessoa, R.S., Maciel, H.S., Massi, M. and Mengui, U.A. (2008) The Effect of Oxygen Concentration on the Low Temperature Deposition of TiO_2 Thin Films. *Surface and Coatings Technology*, **202**, 2126-2131. https://doi.org/10.1016/j.surfcoat.2007.08.075

[14] Löbl, P., Huppertz, M. and Mergel, D. (1994) Nucleation and Growth in TiO_2 Films Prepared by Sputtering and Evaporation. *Thin Solid Films*, **251**, 72-79. https://doi.org/10.1016/0040-6090(94)90843-5

[15] Zhang, Y., Ma, X., Chen, P., Yang, D. and Cryst, J. (2007) Effect of the Substrate Temperature on the Crystallization of TiO_2 Films Prepared by DC Reactive Magnetron Sputtering. *Journal of Crystal Growth*, **300**, 551-554. https://doi.org/10.1016/j.jcrysgro.2007.01.008

[16] Kim, S.H., Choi, Y.L., Song, Y.S., Lee, D.Y. and Lee, S.J. (2002) Influence of Sputtering Parameters on Microstructure and Morphology of TiO_2 Thin Films. *Materials Letters*, **57**, 343. https://doi.org/10.1016/S0167-577X(02)00788-7

[17] Suhail, M.H., Rao, G.M. and Mohan, S. (1992) Dc Reactive Magnetron Sputtering of Titanium Structural and Optical Characterization of TiO_2 Films. *Journal of Applied*

Physics, **71**, 1421-1427. https://doi.org/10.1063/1.351264

[18] Mardare, D. and Stancu, A. (2000) On the Optical Constants of TiO_2 Thin Films. Ellipsometric Studies. *Materials Research Bulletin*, **35**, 2017-2025. https://doi.org/10.1016/S0025-5408(00)00408-6

[19] Pamu, D., Krishna, M.G., Raju, K.C. and Bhatnagar, A.K. (2005) Ambient Temperature Growth of Nanocrystalline Titanium Dioxide Thin Films. *Solid State Communications*, **135**, 7-10. https://doi.org/10.1016/j.ssc.2005.04.003

[20] Swanepoel, R. (1984) Determination of Surface Roughness and Optical Constants of Inhomogeneous Amorphous Silicon Films. *Journal of Physics E*: *Scientific Instruments*, **17**, 896. https://doi.org/10.1088/0022-3735/17/10/023

[21] Shibata, A., Okimura, K., Yamamoto, Y. and Matubara, K. (1993) Effect of Heating Probe on Reactively Sputtered TiO_2 Film Growth. *Japanese Journal of Applied Physics*, **32**, 5666-5670. https://doi.org/10.1143/JJAP.32.5666

[22] Window, B. and Savvides, N. (1986) Electron Stimulated Desorption and Its Relation to Molecular Structure at Surfaces. *Journal of Vacuum Science & Technology A*, **4**, 453. https://doi.org/10.1116/1.573904

[23] Witit-Anun, N., Kasemanankul, Chaiyakun, S., Pokaipisit, A. and Limsuwan, P. (2010) Comparison of Nanocrystalline TiO_2 Films Prepared on Unheated Substrates Using Single- and Dual-Cathode DC Unbalanced Magnetron Sputtering Systems. *Japanese Journal of Applied Physics*, **49**, Article ID: 051101. https://doi.org/10.1143/JJAP.49.051101

[24] Okimura, K., Shibata, A., Maeda, N. and Tachibana, K. (1995) Preparation of Rutile TiO_2 Films by RF Magnetron Sputtering. *Japanese Journal of Applied Physics*, **34**, 4950. https://doi.org/10.1143/JJAP.34.4950

[25] Shakibania, R. (2017) Kinetic Model for Nanocrystalline Anatase to Rutile Polymorphic Transformation. *Chemical and Biochemical Engineering Quarterly*, **31**, 353-359. https://doi.org/10.15255/CABEQ.2017.1094

[26] Tapabrata, D., Sidhartha, S.J. and Dillip, K.P. (2016) Equilibrium State of Anatase to Rutile Transformation for Nano-Structured Titanium Dioxide Powder Using Polymer Template Method. IOP Conference Series: Materials Science and Engineering, Vol. 115.

[27] Wasa, K. and Hayakawa, S. (1993) Handbook of Sputter Deposition Technology: Principles, Technology and Applications. William Andrew, Norwich.